38-075C/96/1618-471-479$03.00/0
il Science

August 1996
Vol. 161, No. 8
Printed in U.S.A.

THERMALLY INDUCED WATER MOVEMENT IN UNIFORM CLAYEY SOIL[1]

I. N. Nassar[2], J. G. Benjamin,[3] and R. Horton[4]

Drying of a soil surface can lead to cracking, thereby creating large channels for waste to leach out of a landfill site. Temperature affects the rate of drying. Water movement induced by thermal gradients was studied with physical experiments using soil columns and with numerical experiments using a computer program. Clay soil material was moistened to 0.407 or 0.392 m^3/m^3 water content. The moistened soil was packed and compacted to a density of 1.45 Mg/m^3 into 0.3-m long columns. The soil columns were closed at the top end using black plastic discs and closed at the bottom end using plexiglas discs. The soil columns moistened at 0.407 m^3/m^3 were subjected to natural radiation for 55 days and those moistened at 0.392 m^3/m^3 were subjected to elevated radiation levels provided by heat lamps for 54 days. Both levels of radiation create periodic temperature boundaries at the ends of soil columns. The numerical model describes coupled heat and water transfer in the soils. The soil columns receiving elevated radiation had more net water movement from the hot ends toward the cold ends of the soil columns than did the soil columns exposed to natural radiation. The model predicted the soil water content distributions well along the soil column compared with the measured water content. The study shows that there may be some drying of compacted soil under a plastic landfill liner as a result of temperatures and thermal gradients created when the liner is exposed to the high periodic temperature regime in comparison with the low periodic temperature regime. The drying was limited to the surface 20 mm. The computer program was also used to simulate the condition of constant boundary temperatures. Temperatures of 50 and 20°C were used at the hot and cold ends, respectively. The numerical study with constant thermal gradients showed that, compared with periodic temperature regimes, large amounts of water migrated. The drying was extended to a depth of 70 mm. Decomposing buried waste that generates heat can lead to a constant thermal gradient in the clay liner. This can cause more severe drying and cracking than a liner surface exposed to the natural periodic heating and cooling of the environment. Generated heat may accelerate deterioration of the plastic liner as well.

THE most effective landfill-liner designs, especially designs for secure disposal of hazardous wastes, combine layers of highly compacted soil or clay with one or more synthetic liners (Peyton and Schroeder 1990). The synthetic liner, usually a black, high-density polyethylene material, has extremely low permeability to prevent leachate from moving out of the landfill. The soil underlying the synthetic liner is compacted to a high bulk density with low permeability to decrease movement from the site of leachate that may penetrate the synthetic liner because of holes or tears. To achieve the high bulk density and low saturated conductivity of the soil liner with the least amount of compacting energy, soil is compacted at the optimum water content (ASTM standard test D-698-78 Method A 1982), which

[1] Contribution from the Agronomy Dept., Iowa State University, Ames IA. Journal Paper no. J-15333 of the Iowa Agric. and Home Econ. Exp. Stn., Ames, IA. Project no. 3262.

Although the research described in this article has been funded wholly or in part by the United States Environmental Protection Agency under assistance agreement (CR818519) to Iowa State University, it has not been subjected to the Agency's peer and administrative review and, therefore, may not necessarily reflect the views of the Agency, and no official endorsement should be inferred.

[2] Faculty of Agriculture, Damnhour, Alexandria University, Egypt.

[3] USDA-ARS, Great Plains Systems Research Unit, Ft. Collins, CO 80522.

[4] Agronomy Dept., Iowa State University, Ames, IA 50011. Dr. Horton is corresponding author. E-mail: rhorton@iastate.edu

Received Oct. 26, 1995; accepted May 2, 1996.

is usually close to the saturated water content of the compacted soil. The landfill site may be prepared several months in advance of filling. During this open period, high temperatures may occur on the surface of the plastic and on the soil surface directly beneath the plastic. A concern arises that drying and cracking of the compacted-soil liner could occur because of moisture movement beneath the plastic liner caused by large temperature gradients. Basnett and Brungard (1992) observed cracks in a clay liner in a landfill site and hypothesized that the cracks were formed by water evaporating from the clay liner and condensing on the under surface of the plastic liner where it migrated down slope. Another mechanism for water movement may be from water vapor movement and/or changes in the water potential and hydraulic conductivity as a result of temperature gradients within the clay liner. In either case, any cracks formed in the compacted-soil liner lessen the effectiveness of the liner by providing pathways for leachate movement out of the landfill site.

Water movement can be caused by thermal gradients within the soil, both by water vapor movement from the warmer to cooler soil zones and by temperature effects on the physical properties of water (Philip and de Vries 1957; de Vries 1958; Milly 1982; Chung and Horton 1987; Scanlon and Milly 1994). Generally, the vapor movement of water from potential gradients and the temperature effects on liquid water movement are ignored for water flux calculations. As shown by Milly (1984a), however, water vapor movement becomes relatively more important for dry soils with extremely low liquid-water conductivities. The temperature affects the water vapor flux through changes in the isothermal water vapor conductivity and thermal water vapor diffusivity. The water vapor conductivity and diffusivity are described, respectively, as:

$$K_{mv} = \theta_a \Omega g \, D_a \rho_v / (\rho_L R T) \quad (1)$$

and

$$D_{TV} = \theta_a \Omega D_a \eta / \rho_L (h d\rho_o / dT - g\rho_v \psi / RT^2) \quad (2)$$

where K_{mv} is the isothermal water vapor conductivity, (m/s), D_{TV} is the thermal water vapor diffusivity, (m^2/s K), θ_a is the air-filled porosity (m^3/m^3), Ω is the tortuosity factor, ρ_L is the density of liquid water (kg/m^3), g is the gravitational constant (m/s^2), D_a is the molecular diffusion coefficient of water vapor in air (m^2/s), ρ_v is the water vapor density in the air phase (kg/m^3), R is the universal gas constant (J/kg K), T is temperature (K), η is a correction factor to account for enhancements of vapor flow attributable to temperature gradients in the air phase (Philip and de Vries 1957), h is the relative humidity, ρ_o is the saturated vapor density (kg/m^3), and ψ is liquid water matric potential (m).

Milly (1984a) also showed that the temperature effects on the physical properties of water should not be ignored for the calculation of water transport in wet soils with large temperature gradients. Temperature affects liquid flow by changing the physical properties of water. Milly (1982) discusses temperature effects on matric potential through changes in water surface tension and density. He gives a matric potential correction as:

$$\Psi_{(\psi,T)} = \Psi\sigma(T_o)\rho_L(T) / (\sigma(T)\rho_L(T_o)) \quad (3)$$

where σ is the surface tension (J/m^2), and T_o is the reference temperature (K). Thermal effects on unsaturated hydraulic conductivity, K, occur through effects on kinematic viscosity, ν, by:

$$K = K(\theta, T) = K(\theta, T_o)\, \nu(T_o) / \nu(T) \quad (4)$$

where $K(\theta, T_o)$ is the unsaturated hydraulic conductivity at water content θ (m^3/m^3) and reference temperature T_o (C), and ν is kinematic viscosity of water (m^2/s).

The objective of this study is to investigate experimentally and numerically the movement of water in compacted soil beneath a plastic liner subjected to large and small temperature gradients. Both constant and periodic temperature gradients are investigated.

MATERIALS AND METHODS

Two types of studies are achieved in the present work. The first represents physical experiments for water distributions under natural radiation and elevated radiation. The second experiment represents numerical studies based upon a coupled heat and water transfer model.

Physical Experiments

The first part of this study made use of a clay soil material. A Clarinda clay (44% clay, 21 sand, 35 silt) (AASHTO classification A-7, Unified classification CH) was collected by excavation, air dried, and ground to pass a 2-mm sieve. The soil has an electrical conductivity of 0.57 dS/m at saturation condition. The small electrical conductiv-

ity results from low concentration of soluble salt. The effect of solute on water flow under the condition of the present study should be insignificant. Two soil batches were moistened using distilled water. The first batch was wetted to 0.281 kg/kg (0.407 m^3/m^3) water content (optimum water content = 0.27 kg/kg), and the second batch was wetted to 0.27 kg/kg (0.392 m^3/m^3) water content. Both soil batches were stored at 20°C for more than 4 days. The soil was packed and compacted into 0.075-m-diam. × 0.30-m-long PVC plastic columns using an Instron Model 1125 controlled hydraulic press, to a 1.45 Mg/m^3 bulk density. Six identical columns were prepared from each batch. After packing, each soil column was sealed at the top with a 0.0015-m thick black plastic disc and closed at the bottom end with a plexiglas disc. Copper-constantan thermocouples were placed at 0.00- (surface of a soil column), 0.02-, 0.05-, 0.10-, 0.15-, 0.20-, 0.25-, and 0.30-m (bottom of a soil column) depths in each column. The thermocouples were located longitudinally at the center of soil columns. The soil columns were buried in a soil pit in a greenhouse, with the top of the column level with the surface of the soil in the pit. The surrounding soil in the pit was covered with the same plastic material used to seal the tops of the columns. Two temperature regimes were imposed on the soil columns. The first temperature regime used natural solar radiation and ambient greenhouse temperatures to create a temperature gradient for soil columns wetted at 0.407 m^3/m^3 water content. Surface temperature amplitudes ranged from 1 to 11°C during the experiment. A second temperature regime used 350-W heat lamps, placed 0.25 m above the soil surface, to provide additional radiation for 12 h during the day time. In the latter regime, the soil columns wetted to moisture content of 0.392 m^3/m^3 were used. The surface temperature amplitude with the supplemental heat was 15 to 16°C. Periodic temperature boundaries were achieved in both temperature regimes. Examples of surface and 0.3-m-depth temperature distributions during the day for each temperature regime are shown in Fig. 1. Three soil columns were removed at 9 and at 55 days after the start of the natural radiation treatment and at 12 and at 54 days after the start of the supplemental radiation treatment. When the soil columns were removed, there were no cracks observed in the soil column. For determination of water content distribution, each column was cut into 0.01-m sections for the top 0.05-m depth and then into 0.02-m sections for the rest of soil column. The gravimetric water content of the soil in each section was determined by drying at 105°C for 24 h.

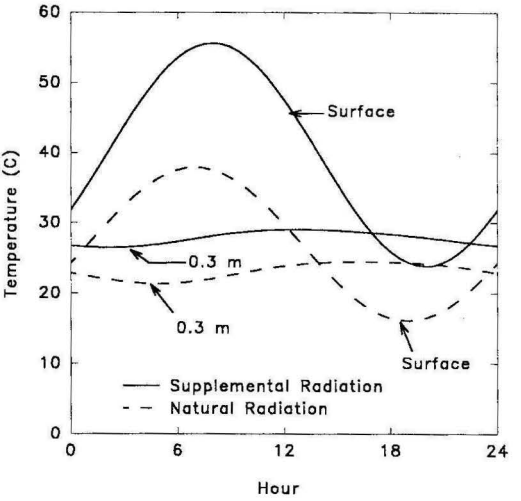

Fig. 1. Daily temperature distributions for the surface and 0.3-m depth for the buried soil columns.

Numerical Experiment

Governing Equations

The theory developed by Milly (1982) for heat and water transfer is used in the one-dimensional form for the present analysis. The theory considers that water (vapor and liquid phases) transfers under gradients of temperature, matric pressure head, and gravity head and that heat transfers by conductive, latent heat, and sensible heat. The following balance equations describe temporal and spatial variations of soil temperature and water content in vertical soil columns. Assuming one-dimensional transfer in the z direction, the nonsteady-state energy balance equation may be written as

$$K_1 \frac{\partial T}{\partial t} + K_2 \frac{\partial \theta}{\partial t} = -\frac{\partial q}{\partial z} \quad (5)$$

where the net heat flux, q, is given in terms of conductive, latent heat, and sensible heat fluxes, respectively, by

$$q = -K_e \frac{\partial T}{\partial Z} - \rho_L L K_{mv} \frac{\partial \Psi}{\partial z} + C_L m_w (T - T_o) \quad (6)$$

where t is time (s), K_e is effective thermal conductivity of soil (W/m K) and m_w is net water flux (kg/m^2 s).

The coefficients K_1 and K_2 of the storage terms in Eq. (5) are given by:

$$K_1 = C_s + [L_o + C_p(T - T_o)]\theta_a \frac{\partial \rho_v}{\partial T} \quad (7)$$

$$K_2 = [L_o + C_p(T - T_o)]\theta_a \frac{\partial \rho_v}{\partial \psi}\frac{\partial \psi}{\partial \theta} + C_L\rho_L(T - T_o) - \rho_L W - C_p\rho_v(T - T_o) - L_o\rho_v \quad (8)$$

The air-filled porosity, θ_a, is the difference between the total soil porosity, P, and the volumetric water content θ. The latent heat of vaporization, L, and the volumetric heat capacity of the wetted soil, C_s, are given, respectively, by

$$L = L_o - (C_L - C_p)(T - T_o) \quad (9)$$

$$C_s = C_d + C_p\rho_v\theta_a + C_L\rho_L\theta \quad (10)$$

where C_d is volumetric heat capacity of dry soil (J/kg), C_L is specific heat of liquid water (J/kg), C_p is specific heat capacity of water vapor (J/kg), L_o is latent heat of vaporization at a reference temperature, T_o, (J/kg), and W is differential heat of wetting (J/kg).

The nonsteady-state mass balance equation for the water flow may be written as

$$(1 - \frac{\rho_v}{\rho_L} + \frac{\theta_a}{\rho_L}\frac{\partial \rho_v}{\partial \psi}\frac{\partial \psi}{\partial \theta})\frac{\partial \theta}{\partial t} + (\frac{\theta_a}{\rho_L}\frac{\partial \rho_v}{T})\frac{\partial T}{\partial t} = -\frac{\partial (m_w/\rho_L)}{\partial z} \quad (11)$$

where the net mass flux of water, m_w, is given by

$$m_w = -\rho_L[(K + K_{mv})\frac{\partial \psi}{\partial z} + (D_{TL} + D_{TV})\frac{\partial T}{\partial z} - Kk] \quad (12)$$

where D_{TL} is the thermal liquid water diffusivity (m^2/s K) and k is a unit vector. The thermal liquid flux was ignored by Milly (1982) because the value of D_{TL} is small in comparison to the other water transport coefficient in dry soil.

The initial conditions associated with the energy and mass balance equations, Eqs. (5), and (11) are given by

$$T(z,0) = T_i, \quad \theta(z,0) = \theta_i, \quad (0 < z < l) \quad (13)$$

where l is soil column length (m). The corresponding boundary conditions are formulated for the case of closed soil. These conditions have to describe different time-dependent temperature functions with no flow of water at both ends of the column. The temperature boundary conditions at both ends can be described by

$$T(0,t) = T_m + \sum_1^n A_n \cos(n\omega t - \phi_n) \; t > 0 \quad (14)$$

$$T(l,t) = T_m + \sum_1^n A_n \cos(n\omega t - \phi_n) \; t > 0 \quad (15)$$

A suitable value of n was found to be 3. n is number of harmonic, T_m is the mean temperature at either end of soil column, A_n is the temperature amplitude of the harmonic wave, ω is the angular frequency, and ϕ_n is the phase shift of the temperature wave harmonic. The boundary conditions for water are given in terms of net mass fluxes by

$$m_w(0,t) = 0, \quad t > 0 \quad (16)$$

$$m_w(l,t) = 0, \quad t > 0 \quad (17)$$

Soil Transport Properties and Parameters

The solution of the energy and mass balance equations, Eqs. (5) and (11), requires exact knowledge of several transport properties and parameters of the soil. The functional relationships, $\psi(\theta)$, between the soil water content, θ, and the matric pressure head ψ and the corresponding function $K(\theta, T_o)$ are usually obtained empirically (Campbell 1974). The following functions are used to describe these relationships:

$$\Psi = \Psi_e(\theta/\theta_s)^{-b} \quad (18)$$

$$K(\theta, T_o) = K_s(\theta/\theta_s)^{2b+3} \quad (19)$$

where b and ψ_e are fitting parameters, and θ_s is saturated volumetric water content. Eq. (18) was fitted to the measured θ for determining b and ψ_e. Table 1 shows values for the fitting parameters and K_s of the Clarinda compacted soil. The enhancement factor was calculated using the following form (Cass et al. 1984):

$$\eta = \zeta + \xi\theta - (\zeta - 1)\exp(-[(1 + \rho/\sqrt{\alpha})\theta]^\gamma) \quad (20)$$

where ζ, ξ, ρ, and γ are empirical coefficients, and α is clay fraction in the soil. Values of these em-

TABLE 1

The values of parameters of Eqs. (18), (19) and (20) for compacted Clarinda soil

Eqs. (18) & (19)	b	Ψ_s (m)	θ_s (m^3/m^3)	K_s (m/s)
	20.049	0.029	0.471	3.1×10^{-9}
Eq. (20)	ζ	ξ	γ	ρ
	8.5	6.0	4.0	2.6

pirical coefficients, which were used in the present study, are given in Table 1. The values of these coefficients depend on soil texture and are given in Cass et al. (1984). Increasing or decreasing the enhancement factor can lead to increasing or decreasing the thermal vapor fluxes, respectively. A small range of 10.3 to 10.9 for this factor was used in the present study. The effective thermal conductivity of the soil, K_e, the volumetric heat capacity of dry soil, C_d, and the differential heat of wetting, W, are generally functions of soil particle size distribution, soil water content, soil bulk density, and soil constituents. Expressions for these functions are given by Milly (1984b).

Numerical Model Development

An implicit finite difference numerical scheme (Smith 1978) was used to discretize and solve the two partial differential equations (PDE), Eqs. (5), and (11), using backward difference formula for the time derivative. With this scheme the value of any variable (T, or θ) at a given time $t+\Delta t$ is not just a function of the values of the variables at the preceding time, t, but also involves the values of all variables at the same time, $t+\Delta t$. This is attributable to the nonlinearity of the PDE produced by the dependence of most coefficients on the two variables themselves. However, a simple linearized finite difference form of the PDE was obtained by including coefficients simply estimated as the arithmetic mean of their values either at the two adjacent nodes or at the two consequent time instants. The resulting system of finite difference equations with 2N unknowns was solved simultaneously for each time step, where N is the number of nodes along the soil column axis. An iteration method was used when solving these equations after arranging them in matrix form. The 2N by 2N coefficient matrix was block-tridiagonal and was efficiently solved by using Gaussian elimination method with backsubstitution. The Gaussian elimination reduces a matrix not all the way to the identity matrix, but only halfway, to a matrix whose components on the diagonal and above remain nontrivial. For a given time instant of order j+1, the values of matrix coefficients were first taken as those for the preceding time of order j. Then a first approximation of values of the 2N variables for the given time instant was obtained. These values were introduced to improve the matrix coefficients and then to obtain new values of the variables. Proceeding in a similar manner, a final solution could be obtained for the given time instant of order j+1 with an arbitrarily chosen accuracy of each variable.

Simulations

The numerical model was used to investigate two liner conditions: periodic heating and cooling, and constant heating. The periodic heating and cooling condition represents a liner exposed to natural radiation. The constant heating represents a buried liner in contact with heat generating decomposing waste. For periodic conditions the numerical model was used to predict water content distributions in the compacted Clarinda clay soil and to calculate the isothermal/thermal water flux ratio at 0.04-m depth from the top of soil columns. The predicted values were compared to the measured water content distributions from the physical experiments. For constant heating conditions the model was used to simulate effects of constant boundary temperatures on water movement under plastic liners. The simulation was performed using the soil properties of compacted Clarinda soil along with temperatures of 20 and 50°C at the cold and hot ends, respectively. The initial water content and simulation time were 0.392 m^3/m^3 and 54 days, respectively. A mass balance for the water of soil columns was calculated from the measured and predicted water content distributions. The mass balance was calculated for the small and large temperature amplitudes at the final days. The measured and calculated mass balances for small temperature amplitudes were 0.11447 and 0.11427 m, respectively, and for the large temperature amplitude were 0.10998 and 0.10988 m, respectively.

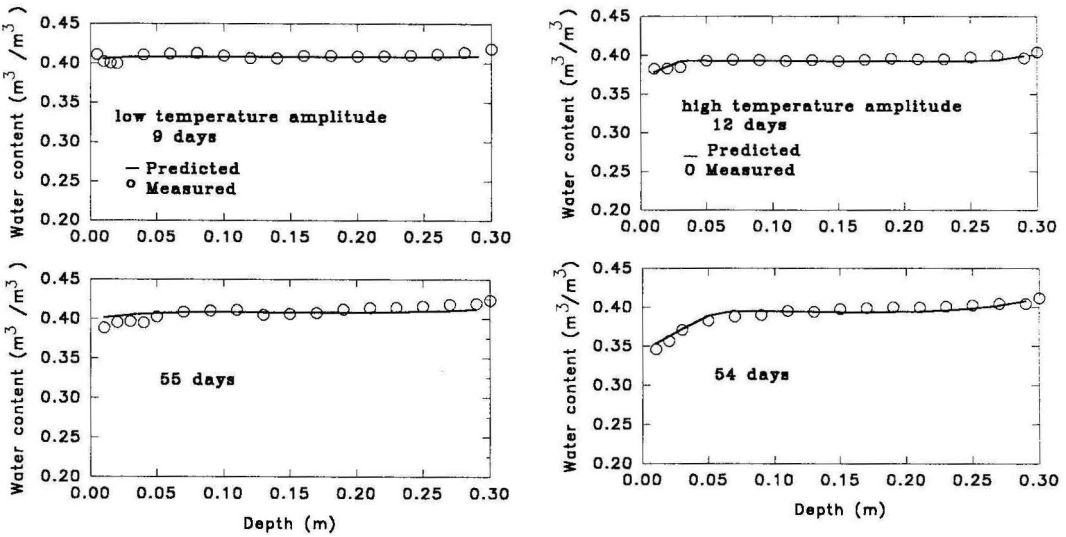

Fig. 2. Measured and predicted water-content distributions for the buried soil columns, low temperature (a) and high temperature amplitudes (b).

RESULTS AND DISCUSSION

The isothermal water vapor conductivity (K_{mv}) and thermal water vapor diffusivity (D_{Tv}), and the correction factors for matric potential and hydraulic conductivity, are shown in Table 2. Although K_{mv} is three to four orders of magnitude smaller than D_{Tv}, the contribution of the isothermal water vapor conductivity to the isothermal water flux also depends upon the matric potential gradient. K_{mv} is about 4 orders of magnitude smaller than the saturated hydraulic conductivity for the compacted Clarinda soil (3 10^{-9} m/s), but it should not be ignored for the calculation of water movement under plastic liners. Vapor diffusion may be more important for soils with lower liquid-water hydraulic conductivity, such as those used by Horton et al. (1987). The effect of temperature on hydraulic conductivity, through effects on viscosity, is greater than the effects of temperature on matric potential, through effects on surface tension. The hydraulic conductivity more than doubles with a change of temperature from 20 to 60°C, whereas the change of matric potential is only about 8%.

The measured and predicted water-content distributions under natural radiation conditions (Fig. 2a) showed little net water movement caused by thermal gradients. For the supplemental radiation treatment, water content of the surface, warm end of the soil column, was about 0.07 m^3/m^3 less than the buried, cooler end of the soil column (Fig. 2b). For the natural radiation treatment the difference in the water content for the corresponding ends was 0.03 m^3/m^3. The model also predicted a drier soil near the surface of the warm end of the soil for the supplemental radiation. Both the measurements and the model showed the drying to be limited to the top 20

TABLE 2

Isothermal water vapor conductivity, K_{mv} (m/s), and thermal water vapor diffusivity, D_{TV} (m^2/s C), for compacted Clarinda soil at θ of 0.407 m^3/m^3; and temperature correction factors for matric potential, $\sigma(T_o)\,\rho_l(T) / (\sigma(T)\,\rho_l(T_o))$[a], and hydraulic conductivity, $\nu(T_o) / \nu(T)$[a].

	Temperature (°C)			
	5	20	35	50
K_{mv}	$6.8\ 10^{-17}$	$1.8\ 10^{-16}$	$4.4\ 10^{-16}$	$1.2\ 10^{-15}$
D_{TV}	$4.7\ 10^{-13}$	$1.8\ 10^{-12}$	$3.3\ 10^{-12}$	$6.4\ 10^{-12}$
$\sigma(T_o)\,\rho_L(T) / \sigma(T)\,\rho_L(T_o)$	0.97	1.00	1.03	1.08
$\nu(T_o) / \nu(T)$	0.65	1.00	1.40	2.18

[a] Temperature effects on surface tension, density and viscosity of liquid water are for pure, free water.

and 70 mm, respectively, for low and high temperature amplitudes. The thermal vapor flux is large for the high temperature columns compared with the low temperature soil columns. The thermal vapor flux increases as the thermal water vapor diffusivity increases (Table 2) and as the thermal gradients increase. The results in this study are in agreement with results provided by Vielhaber et al. (1994). They reported that water movement in soil liners is primarily caused by variation in both temperature and temperature gradients. To minimize the possibility of drying and cracking of the soil underlying the plastic liner, the liner should not be exposed to large surface radiation for extended periods of time. The liner should be shaded after being placed.

Predicted water redistribution in response to constant boundary temperatures is shown in Fig. 3 for two different periods (12 and 54 days). The water migrated from the hot end (high temperature boundary) toward the cold end (low temperature boundary) during the two periods. The amount of migrated water increased as time increased. The net water transfer with the constant boundary temperatures was great compared with the net water transfer with the natural and elevated radiation (Figs. 2a and b). Buried waste that generates heat as a result of chemical decomposition or radiative decay can provide heat flux over a long period of time. This can result in a constant thermal gradient. The water vapor moves continuously from hotter to cooler soil. The water vapor condenses at the cooler region of soil producing a matric potential gradient that circulates liquid water back upward. The solar radiation heating and cooling is not a constant. During part of the day, the temperature gradient decreases downward, and during cooling it reverses direction. Water moves downward and then back up again in a cyclic manner.

Figure 4 shows the absolute isothermal/thermal water flux ratio as a function of time for periodic large temperature amplitude. The ratio is calculated at times of 8 a.m. and 2 p.m. on consecutive days for the 0.04-m depth. The ratio reveals that isothermal water flux increases with time. The increase is due to an increase of the matric potential gradient as time increases. The ratio is less than unity indicating that net water transfer was always toward the bottom end of the soil column. The isothermal flux during the first 6 days was negligible but it was close to unity during the last 6 days. Because the temperature gradient is smaller at 8 a.m. than at 2 p.m., this results in a greater ratio at 8 a.m. than at 2 p.m. The differences in the ratio between times 8 a.m. and 2 p.m. increase as time increases. The values of the ratio for Day 52 were 0.852 and 0.243 at 8 a.m. and 2 p.m., respectively.

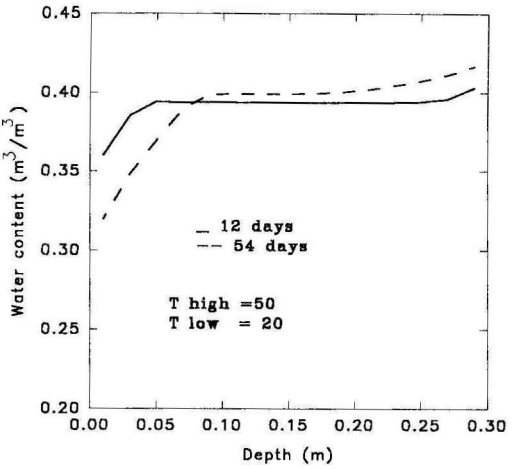

Fig. 3. Predicted water-content distributions for compacted Clarinda soil under constant boundary temperatures.

Figure 5 shows predicted water distribution for small and large periodic boundary temperatures, and constant boundary temperatures. The initial water content for the three temperature boundaries was the same (0.392 m^3/m^3). In all cases the lower depths showed increases in water content, reflecting the drying of the near surface zones. The soil surface dried relatively quickly in the constant boundary temperature, from a soil water content of 0.392 to a water content of 0.340 m^3/m^3 in only about 7 days. In the case of large amplitude periodic temperature boundary, the soil surface dried from 0.392 to 0.365 m^3/m^3 in approximately 15 days. In the case of small am-

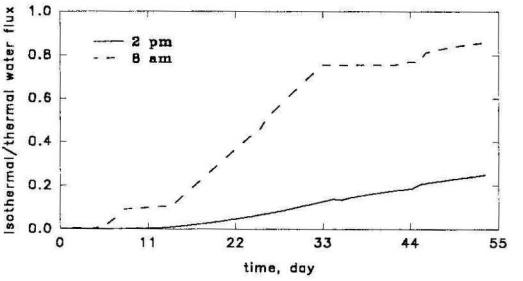

Fig. 4. Predicted ratio of absolute isothermal/thermal water flux at depth of 0.04 m. The ratio is graphed at times of 8:00 a.m. and 2:00 p.m. on consecutive days.

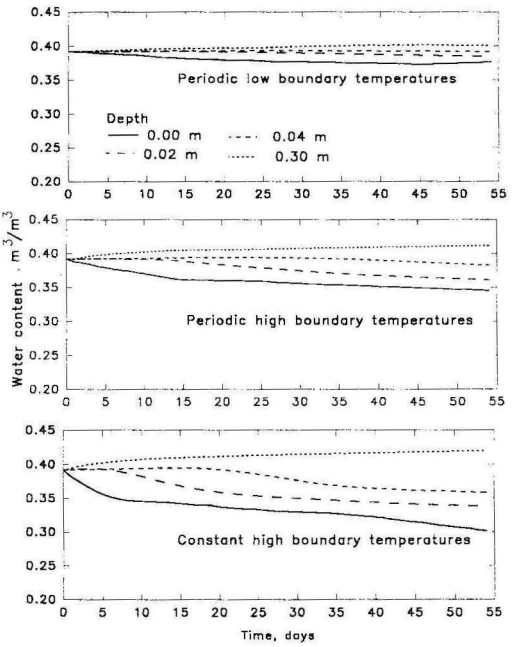

Fig. 5. Predicted water-contents through time at selected depths for soil under low and high boundary temperatures, and constant boundary temperatures.

plitude periodic temperature boundary, the surface water content decreased from 0.392 to 0.38 in 15 days. For constant boundary temperatures, soil drying extended to deeper depths than occurred with either small or large amplitude periodic temperature boundaries. For example, water initially at a depth of 40 mm did move down toward the cold end under the constant temperature boundaries, but it did not indicate movement for either the small or large amplitude periodic temperature conditions. With a constant thermal gradient, water transfers, mostly in vapor phase, in one direction toward the cold end of soil column; after condensation some water moves back in liquid form toward the warm end of soil column. In the presence of a periodic temperature gradient, water moves toward the bottom end of a soil column during the day and moves back toward the soil column surface at night. Values of water content at zero depth reveal that steady-state water flux occurred after 35 and 45 days for small and large temperature amplitudes, respectively. However, under constant temperature, the surface layer continues to lose water even at day 55. It can be concluded that the net water transfer under periodic temperature gradients must be less than under constant temperature gradients. This study shows that the compacted soil under a plastic landfill liner may dry slowly because of periodic thermal gradients caused by solar radiation, but enhanced drying is shown for constant thermal gradients when the liner is exposed to heat generated from buried chemical or radiative wastes. The results of periodic temperature reveal that exposing a flat clay liner covered with plastic to natural radiation may not cause severe drying for the liner. However, for a sloping liner covered with plastic, water vapor may condense on the bottom of the plastic cover enabling water seepage to occur on the underside of the plastic. For this condition severe desiccation and cracking of the clay liner may cause a problem in the liner management (Basnett and Brungard, 1992).

NOTATION

A_n temperature amplitude [°C, K]
b fitting coefficient defined in Eqs.(18)and (19)
C_d volumetric heat capacity of dry soil [J m^{-3} K^{-1}]
C_L specific heat of liquid water [J kg^{-1} K^{-1}]
C_p specific heat of water vapor at constant pressure [J kg^{-1} K^{-1}]
C_s volumetric heat capacity of wetted soil [J m^{-3} K^{-1}]
K_{mv} isothermal water vapor conductivity [m s^{-1}]
D_{TL} thermal liquid water diffusivity [m^2 s^{-1} K^{-1}]
D_{TV} thermal water vapor diffusivity [m^2 s^{-1} K^{-1}]
g gravitational acceleration [m s^{-2}]
K unsaturated hydraulic conductivity [m s^{-1}]
$K(\theta,T_o)$ unsaturated hydraulic conductivity measured at water content θ ant reference temperature T_o [m s^{-1}]
K_s saturated hydraulic conductivity [m s^{-1}]
k unit vector opposite gravity
K_e effective thermal conductivity of the soil [W m^{-1} K^{-1}]
L latent heat of vaporization [J kg^{-1}]
L_o latent heat of vaporization at reference temperature [J kg^{-1}]
l soil column height [m]
m_w net mass flux of water [kg m^{-2} s^{-1}]
q net heat flux [W m^{-2}]
P total soil porosity
R universal gas constant [J kg^{-1} K^{-1}]
T soil temperature [°C, K]
T_i initial soil temperature [°C, K]
T_m mean temperature defined in Eqs. (14 and 15) [°C, K]
T_o reference temperature [°C, K]
t time [s]
W differential heat of wetting [J kg^{-1}]
z vertical ordinate in the downward direction [m]

GREEK SYMBOLS

α clay fraction in soil
θ volumetric water content in the liquid phase
θ_a air-filled porosity [m^3/m^3]
θ_i initial volumetric water content in the liquid phase
θ_s saturated volumetric water content in the liquid phase ν dynamic viscosity of water [$m^2 s^{-1}$]
η enhancement factor for thermal vapor flux
ρ_l density of liquid water [kg m^{-3}]
ρ_v water vapor density [kg m^{-3}]
ζ empirical coefficient in Eq. (20)
ξ empirical coefficient in Eq. (20)
γ empirical coefficient in Eq. (20)
ρ empirical coefficient in Eq. (20)
ϕ_n phase shift of the temperature wave harmonic [rad]
ψ matric pressure head measured at reference temperature [m]
ψ matric pressure head as a function of T and θ [m]
ψ_e air entry matric pressure head [m]
ω angular frequency [rad s^{-1}]
σ surface tension [J/m^2]
Ω tortuosity factor

REFERENCES

ASTM D-698-78 Method A. 1982. Standard test methods for moisture-density relations of soils and soil-aggregate mixtures using 5.5-lb. (2 49-kg) hammer and 12-inch (305-mm) drop. Annual book of ASTM standards. Part 19. Soil and rock; building stones, American Society for Testing and Materials, Philadelphia, PA, pp. 202-208.

Basnett, C., and M. Brungard. 1992. The clay desiccation of a landfill composite lining system. Geotechical Fabrics Report, Jan./Feb., 38-41.

Campbell, G. C. 1974. A simple method for determining unsaturated conductivity from moisture retention data. Soil Sci. 117:311-314.

Cass, A., G. S. Campbell, and T. L. Jones. 1984. Enhancement of thermal water vapor diffusion in soil. Soil Sci. Soc. Am. J. 48:25-32.

Chung, S. O., and R. Horton. 1987. Soil heat and water flow with a partial surface mulch. Water Resour. Res. 23:2175-2186.

de Vries, D. A. 1958. Simultaneous transfer of heat and moisture in porous media. Trans. Am. Geophys. Union 39:909-916.

Horton, R., M. L. Thompson, and J. F. McBride. 1987. Method of estimating the travel time of noninteracting solutes through compacted soil material, Soil Sci. Soc. Am. J. 51:48-53.

Milly, C. P. D. 1982. Moisture and heat transport in hysteretic, inhomogeneous porous media: A matric head-based formulation and a numerical model. Water Resour. Res. 18:489-498.

Milly, C. P. D. 1984a. A linear analysis of thermal effects on evaporation from soil. Water Resour. Res 20:1075-1085.

Milly, C. P. D. 1984b. A simulation analysis of thermal effects on evaporation from soil. Water Resour. Res.20:1087-1098.

Peyton, R. L. and P. R. Schroeder. 1990. Evaluation of landfill-liner designs, J. Environ. Eng. 116:421-437.

Philip, J. R., and D. A. de Vries. 1957. Moisture movement in porous materials under temperature gradients, Trans. Am. Geophys. Union 38:222-232

Scanlon, B. R. and P. C. D. Milly. 1994. Water and heat fluxes in desert soils: 2. Numerical simulations. Water Resour. Res. 30:721-733.

Smith, G. D. 1978. Numerical solution of partial differential equations: Finite difference methods. 2nd Ed. Clarendon Press, Oxford, UK.

Vielhaber, B., S. Melchior, K. Berger, and G. Miehlich. 1994. Field studies on the thermally induced desiccation risk of cohesive soil liners below geomembranes in landfill covers. *In* In-situ remediation: Scientific basis for current and future technologies, Part 1. G. W. Gee and N. R. Wing (eds.). Proceedings of the Thirty-Third Hanford Symposium on Health and the Environment, November 7-11, 1994, Pasco, Washington. Battelle Press, Columbus, OH.